(Preprint) AAS 14-365

# ROUND-TRIP SOLAR ELECTRIC PROPULSION MISSIONS FOR MARS SAMPLE RETURN

Zachary J. Bailey,[*] Erick J. Sturm,[†] Theresa D. Kowalkowski[‡], Robert E. Lock[§], Ryan C. Woolley[**] and Austin K. Nicholas[††]

Mars Sample Return (MSR) missions could benefit from the high specific impulse of Solar Electric Propulsion (SEP) to achieve lower launch masses than with chemical propulsion. SEP presents formulation challenges due to the coupled nature of launch vehicle performance, propulsion system, power system, and mission timeline. This paper describes a SEP orbiter-sizing tool, which models spacecraft mass & timeline in conjunction with low thrust round-trip Earth-Mars trajectories, and presents selected concept designs. A variety of system designs are possible for SEP MSR orbiters, with large dry mass allocations, similar round-trip durations to chemical orbiters, and reduced design variability between opportunities.

## INTRODUCTION

Mars Sample Return (MSR) has long been a goal of the planetary science community, and was identified as the top priority in the 2011 Decadal Survey.[1] The currently proposed MSR architecture is decomposed into three missions: a caching rover mission (to be launched in 2020)[2], a lander or rover equipped with a Mars Ascent Vehicle (MAV), and an orbiter to collect the sample and return it to Earth.[3]

Previous concepts for MSR orbiters from 2003[4] and 2011[3] have utilized chemical propulsion to achieve the $\Delta V$ required for round-trip travel between Earth and Mars. This architectural decision has led to either very high launch masses or the inclusion of more exotic technologies, such as aerocapture (in the case of the 2003 concept), to reduce launch mass. Solar Electric Propulsion (SEP) provides an alternate method to reduce the launch mass of a MSR orbiter.

[*]Systems Engineer, Pre-Projects Systems Engineering Group, Jet Propulsion Laboratory, California Institute of Technology, M/S 321-250, 4800 Oak Grove Drive, Pasadena, CA 91109.
[†]Systems Engineer, Pre-Projects Systems Engineering Group, Jet Propulsion Laboratory, Laboratory, California Institute of Technology, M/S 321-250, 4800 Oak Grove Drive, Pasadena, CA 91109.
[‡‡]Mission Design Engineer, Outer Planet Mission Analysis Group, Jet Propulsion Laboratory, Laboratory, California Institute of Technology, M/S 301-121, 4800 Oak Grove Drive, Pasadena, CA 91109.
[§]Systems Engineer, Mars Program Formulation Office, Jet Propulsion Laboratory, Laboratory, California Institute of Technology, M/S 321-690, 4800 Oak Grove Drive, Pasadena, CA 91109.
[**]Mission Design Engineer, Inner Planet Mission Analysis Group, Jet Propulsion Laboratory, Laboratory, California Institute of Technology, M/S 301-165, 4800 Oak Grove Drive, Pasadena, CA 91109.
[††]Systems Engineer, Pre-Projects Systems Engineering Group, Jet Propulsion Laboratory, California Institute of Technology, M/S 301-165, 4800 Oak Grove Drive, Pasadena, CA 91109.

A growing number of planetary missions have demonstrated the usefulness of SEP: Deep Space 1, a 1998 NASA technology demonstration mission[5]; SMART-1, a 2003 ESA mission to the Moon[6]; Hayabusa, a JAXA sample return mission to the asteroid Itokawa[7]; and Dawn, a 2007 NASA mission to the asteroid Vesta and dwarf planet Ceres[8]. A 2009 study by Oh *et al.* showed that a SEP-based architecture for a Mars Sample Return has many benefits when compared to a chemical propulsion-based architecture.[9] When compared to the total mission timeline of a chemical mission that includes an aerobraking phase, a SEP mission is comparable in duration. Furthermore, a SEP system could deliver and return larger payload masses to Mars and Earth in a round-trip mission than those of a chemical system on the same launch vehicle.

The use of SEP adds additional complexity in the formulation phase of a mission due to the tightly-coupled interactions between the launch vehicle performance, propulsion system sizing, power system sizing, propellant sizing, mission design, and time-of-flight (TOF).[10] This paper explores the interactions between these parameters, specifically for a MSR orbiter mission, outlines how margin can be applied to a SEP MSR orbiter, and presents results from a newly developed MSR orbiter-sizing tool.

## ASSUMPTIONS

All the SEP mission concepts and trajectories presented in this paper use a commercially available Hall-effect thruster developed by Aerojet, the BPT-4000. Both Hofer and Oh, *et al.* have demonstrated the BPT-4000 to have a superior TOF performance, power capability, and mass throughput compared to other Hall-effect or Ion thrusters for the MSR mission.[9,11] The BPT-4000 is also a highly developed thruster with recent flight heritage on the US Air Force's Advanced Extremely High Frequency (AEHF) communications satellites.[12]

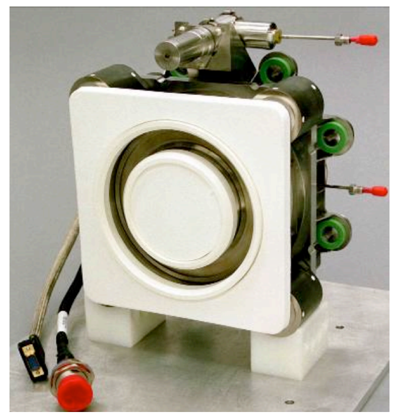

**Figure 1. Aerojet's BPT-4000 Hall-Effect Thruster**

The trajectories discussed in this paper and used in the orbiter-sizing tool are based on work by Kowalkowski *et al.*,[13] which developed a database of Earth-to-Mars (outbound) and Mars-to-Earth (inbound) trajectories using the Mission Analysis Low Thrust Optimization (MALTO) software[14].

## SEP MARGIN ANALYSIS

A Mars mission utilizing SEP has special challenges compared with traditional chemical propulsion architectures, due to the tight coupling of many mission and system parameters. Designing a mission with robust system margins is complicated by this fact. While power and mass margins are relatively independent parameters for a chemical-propulsion orbiter, technical margins are highly coupled and tradable against one another for a SEP mission. This leads to a large degree of flexibility for SEP missions in both the development and operations phases, but requires extra consideration.

The Dawn project recognized this strong coupling of technical resources and margins for a SEP mission.[15] We have used an updated margin method informed by the work on Dawn and updated by Oh, *et al*.[16] In addition to mass and power margins, a SEP mission must track thruster duty-cycle, time-of-flight, and propellant margin. The following sub-sections define and describe the several margins that are tracked by the orbiter-sizing tool.

**Mass Margin**

The mass margin for a SEP mission is tracked against the spacecraft dry mass. The mass margin is defined in Equation (1).

$$m_{Mass} = \frac{M_{Dry,MEV}}{M_{Dry,CBE}} - 1 \tag{1}$$

Where $M_{Dry,CBE}$ is the current best estimate for the spacecraft dry mass, and $M_{Dry,MEV}$ is the maximum expected spacecraft dry mass. For a SEP mission we use standard JPL practices for the mass margin, with a prescribed value of 43% for a pre-PDR concept design.

**Power Margin**

The definition of power margin for a SEP system is somewhat more complicated than mass margin due to the change in available power as a function of heliocentric distance. We begin by defining the several power values of interest for the system. The solar array design has an initial power value at the beginning-of-life (BOL) and at 1AU solar distance, $P_{SA}^{BOL}$. Degradation occurs in the solar array over the course of the mission. For the purposes of simplicity, this degradation is assumed to be 11% of the BOL power. This power degradation is subtracted from the BOL power to arrive at a 1 AU end-of-life (EOL) power value, $P_{SA}^{EOL}$, as shown in Equation (2). This value, $P_{SA}^{EOL}$, is used as the input value to the MALTO trajectory software.[14] We subtract the margined spacecraft bus power from the EOL solar array power to get the un-margined power available for SEP, $P_{SEP}$ (see Equation (3)).

$$P_{SA}^{EOL} = P_{SA}^{BOL} - P_{Degredation} \tag{2}$$

$$P_{SEP} = P_{SA}^{EOL} - P_{Bus}^{M} \tag{3}$$

A constant-percentage power margin is applied to $P_{SEP}$ to get the margined power available for SEP, $P_{SEP}^{M}$, as shown in Equation (4). This study uses a constant value of 30% for $m_{SEP}$ in the examples given in later sections.

$$P_{SEP}^{M} = \frac{P_{SEP}}{1 + m_{SEP}} \tag{4}$$

$$P_{PPU} = min[4.8\ kW, P_{SEP}^{M}] \tag{5}$$

The input power to the power-processing unit (PPU), $P_{PPU}$, given by Equation (5), varies with the power available for SEP. For a BPT-4000 Hall-effect thruster, the maximum PPU input power is 4.8 kW. If the power available for SEP is greater than the maximum PPU power, the excess power will be shunted. Below the PPU power saturation limit, the entire power available for SEP may be used by the PPU. This results in a SEP power margin, Equation (6), which varies with heliocentric distance, since the solar array power, and thus the power available for SEP vary with range from the sun.

$$m_{Power,SEP}(r) = \frac{P_{SEP}(r)}{P_{PPU}} - 1 = max\left[\frac{P_{SA}^{EOL}(r) - P_{Bus}^{M}}{4.8\ kW} - 1, m_{SEP}\right] \tag{6}$$

Figure 2 shows the variation of the several power values and the SEP power margin (black line) as a function of heliocentric distance, for an example, 1-thruster case with a 12 kW EOL solar array, and a 30% power margin. While the SEP power margin is high at launch due to the large amount of unused solar array power, it quickly converges to the prescribed 30% value as the PPU becomes un-saturated.

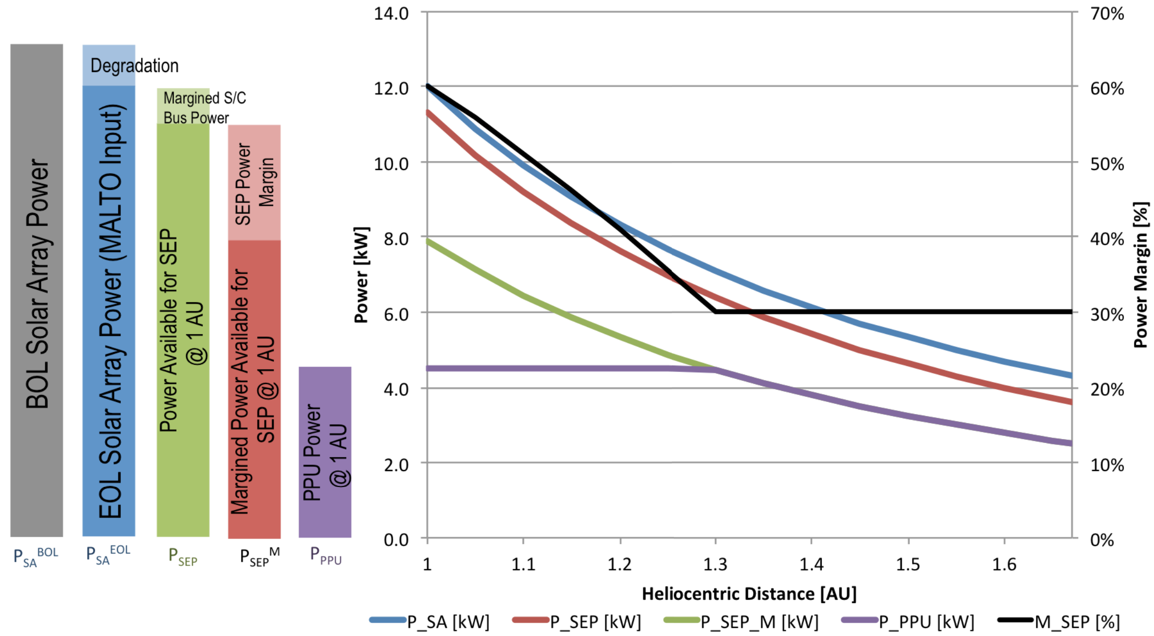


**Figure 2. (L) System power values identified. (R) Power values vs. heliocentric distance. SEP Power margin decreases to a constant value with increasing heliocentric distance.**

### Duty Cycle

Duty-cycle represents a margin that is required to account for periods during the trajectory when the spacecraft is not thrusting (including communication periods, safe mode, science observations, calibration, etc.). For this study a 95% duty-cycle was used as an input parameter to MALTO and was not varied for any cases.

### Propellant Margin

The MALTO trajectory software models the performance of the BPT-4000 thruster with curves of thrust, ISP, and mass-flow-rate vs. PPU input power. These curves account for the thruster & PPU efficiency, but do not include margin on propellant flow rate or thrust.

There are other sources of propellant uncertainty[17], which Oh, *et al.*[16] recommend be covered by a 10% margin on the Xenon propellant mass. Due to the trade-ability of these margin parameters against one another (as described in the "Integrated Margin Approach" section below), we have elected to maintain a higher than recommended power margin of 30% (compared to the 15% recommendation of Oh, *et al.*[16]) to account for these propellant uncertainties.

If a propellant margin were to be applied, the excess margined propellant mass would be added as a residual mass to the Earth-arrival mass, and propagated through the $\Delta V$ budget. Because propellant margin is effectively added to neutral mass (defined as spacecraft dry mass plus any unused propellant at Earth), the available neutral mass headroom in the trajectory limits the amount of propellant margin that may be accommodated.

### Time-of-Flight Margin

While time-of-flight (TOF) is not typically a margined value for traditional chemical propulsion missions, it is an important parameter for SEP missions, since TOF can vary with different values of $P_{SEP}$ and spacecraft neutral mass. Some missions may explicitly track a TOF margin, but this is not necessary for an MSR orbiter mission. In this case, rendezvous dates with Mars and Earth are not fixed, but allowed to float with trajectory selection in order to optimize for spacecraft mass. Time-of-flight is discussed as a figure-of-merit later in this paper.

**Integrated Margin Approach**

In order to help better understand how these margin values interact with one another, we developed a new visualization tool for round-trip Mars SEP missions. The carpet-plot, shown in Figure 3, overlays contours of "power available for SEP" and "total time-of-flight" vs. spacecraft neutral mass and propellant mass. Recall that spacecraft neutral mass is defined as dry mass + chemical propellant mass, and total TOF is the sum of outbound and inbound TOFs. The general trends in this carpet-plot are that for a given neutral mass, lower power levels require more SEP propellant and longer TOFs.

Also plotted in Figure 3 are points that indicate how a notional, un-margined spacecraft would grow as mass, power, and propellant margins are sequentially applied. The first black diamond indicates an un-margined spacecraft design, with an 800 kg neutral mass and 12 kW power. The resultant Xenon propellant mass for the un-margined design is 795 kg.

After applying a nominal 43% mass margin, the neutral mass increases by 345 kg to 1145 kg. Keeping the same un-margined 12 kW power value (and staying on the 12 kW power contour), this heavier neutral mass now requires an additional 265 kg of propellant, and the round-trip TOF has also increased by nearly 200 days. This design point is indicated by the green square.

Applying a notional 15% power margin results in de-rating the power to approximately 10.5 kW. We now read off the propellant mass from a 10.5 kW power contour. This design, indicated by the blue triangle, requires an additional 30 kg of propellant mass.

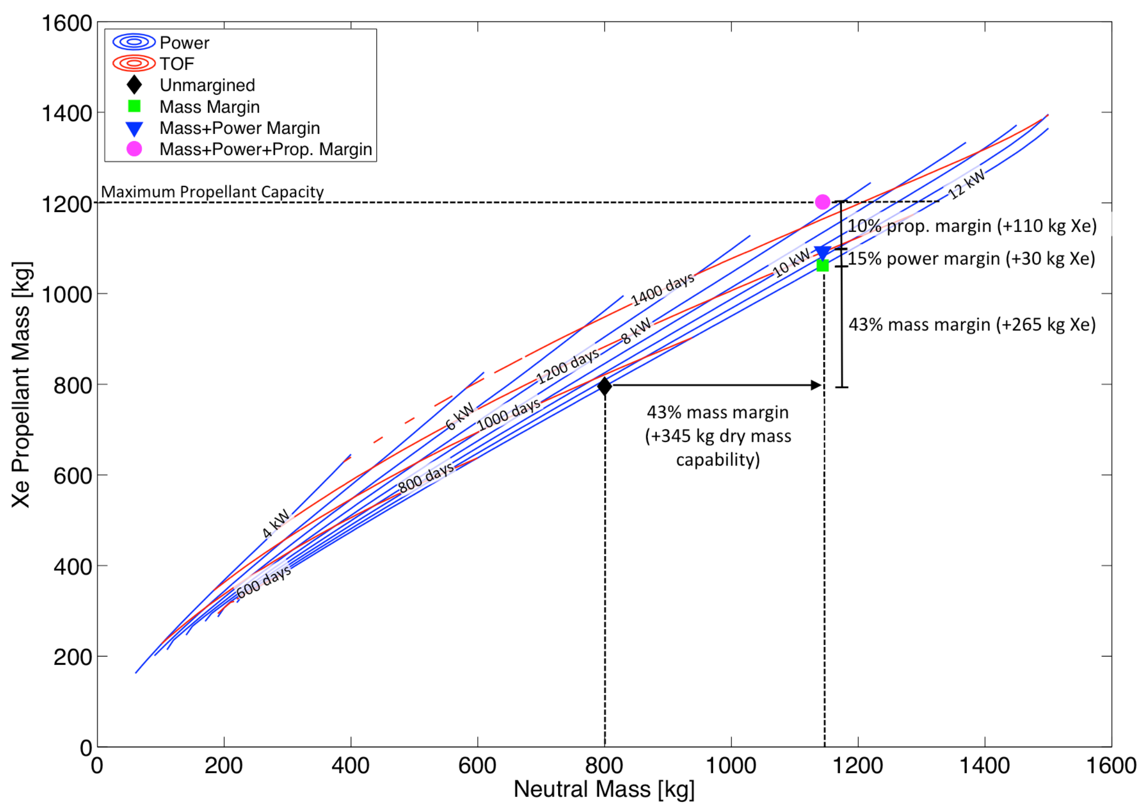


**Figure 3. Carpet plot for a 2022 launch, 2028 return, round-trip SEP mission**

Finally, we apply a propellant margin of 10% to the design, indicated by the magenta circle. This design requires an additional 110 kg, and has increased the total TOF to ~1500 days compared to the <1000 day time in the un-margined case.

By carefully examining this plot, however, one can see how these three margin values are trade-able with one another. In this example, if the power margin is set to 0%, the total propellant load contains 13% propellant margin and 43% mass margin. Similarly, if no power or propellant margin is consumed during the spacecraft development, the spacecraft mass could grow by up to ~70% (to 1350 kg) before a 12 kW power system would require more than the propellant load computed for this example. This method can also be used to re-assess margins quickly as design mature, margin requirements are reduced in later design phases, and as problems occur.

## ORBITER-SIZING TOOL

In order to better understand the effects of the tightly coupled sub-system interactions inherent in a SEP spacecraft, we have developed a multidisciplinary modeling tool that can be used to explore designs for SEP MSR spacecraft in a formulation environment. This tool consists of several elements that pass data back and forth between one another to converge on a spacecraft design. The key elements of this tool are: a trajectory database; a $\Delta V$ calculator; a spacecraft mass model; a launch vehicle model; a mission timeline model; and mass, power, and propellant margin models.

This tool builds on work by Kowalkowski *et al.,*[13] which developed a database of Earth-to-Mars (outbound) and Mars-to-Earth (inbound) trajectories using the MALTO software[14]. A more detailed description of each of the key elements of the orbiter-sizing tool can be found in the following sub-sections. Figure 4 is a design structure matrix (DSM) for the tool, showing all the models and data interconnections between them. The spacecraft, trajectory, and other models have been developed in Excel and Matlab; the integrated SEP MSR orbiter tool is built using Phoenix Integration's ModelCenter tool. ModelCenter allows all of these models to be iterated in order to converge on a feasible spacecraft design for a given set of inputs.

### Spacecraft Sub-System Models

A collection of models is combined to perform the spacecraft mass sizing in this tool. These models and their interconnections are highlighted in the green region in Figure 4. The canonical spacecraft subsystems are represented in these models: Attitude Determination & Control (ADCS), Command & Data Handling (CDHS), Telecom, Power, Propulsion, Thermal, and Mechanical. The ADCS, CDHS, & Telecom models simply report a subsystem mass using analogy-based estimates from user-selectable historical or in-development spacecraft (MAVEN, InSight, MRO, Odyssey, SMAP, & DAWN). The power subsystem uses this method for the non-solar array portion of the power subsystem mass, and includes a solar-array mass sizer, based on the solar array power requirement. The propulsion subsystem model estimates tank mass based on the propellant requirements, and SEP & chemical thruster masses based on relevant component data. The thermal and mechanical subsystem models estimate mass based on weighted fractions of the spacecraft and subsystem masses. A master equipment list (MEL) module determines the total dry & wet spacecraft masses based on the subsystem and propellant masses.

### Earth-to-Mars (Outbound) Trajectories

Mission design is a key element of a SEP mission concept, as it influences the maximum delivered mass, required propellant, required power, and required launch vehicle performance. In order to quickly explore the trade space of SEP orbiters for MSR, a large database of outbound trajectories was developed, as described in Kowalakowki *et al.*[13] Figure 5 shows an example of

| Input: \ Output: | Design Inputs | Outbound Trajectory | Inbound Trajectory | DeltaV Budget | Launch Vehicle | Power & Mass Margin | Propellant Margin | Margined Outbound Trajectory | Margined Inbound Trajectory | Margined DeltaV Budget | Margined Launch Vehicle | Residual Propellant | Solar Array Power | CDHS | ADCS | Telecom | Power | Propulsion | Thermal | Mechanical | MEL | Timeline |
|---|---|---|---|---|---|---|---|---|---|---|---|---|---|---|---|---|---|---|---|---|---|---|
| **Design Inputs** | | 3 | 2 | 2 | | 4 | 1 | | | 1 | | | | 1 | 1 | 5 | 3 | 2 | 1 | 3 | 2 | 1 |
| **Outbound Trajectory** | | | | 3 | 2 | | | 2 | | | | | 1 | | | | | 1 | | | | |
| **Inbound Trajectory** | | | | 2 | | | | | | | | | 1 | | | | | | | | | |
| **DeltaV Budget** | | 1 | 1 | | | | | | | | | 3 | | | | | | | | | | |
| **Launch Vehicle** | | | | | | | | | | | | | | | | | | | | | 2 | |
| **Power & Mass Margin** | | | | | | | | 1 | 1 | 1 | 2 | | | | | | | | | | | |
| **Propellant Margin** | | | | | | | | | | 1 | 1 | | | | | | | | | | | |
| **Margined Outbound Trajectory** | | | | | | | | | | 2 | 2 | | 1 | | | | | | | | | 3 |
| **Margined Inbound Trajectory** | | | | | | | | | | 2 | | | 1 | | | | | | | | | 3 |
| **Margined DeltaV Budget** | | | | | 1 | 1 | 1 | 1 | 1 | | 1 | 3 | | | | | | 3 | | 1 | 2 | |
| **Margined Launch Vehicle** | | | | | | | | | | | | | | | | | | | | | | |
| **Residual Propellant** | | | | 1 | | | | | | | | 1 | | | | | | | | | | |
| **Solar Array Power** | | 1 | 1 | | | | | 1 | 1 | | | | | | | | 1 | | | | | |
| **CDHS** | | | | | | | | | | | | | | | | | | | | 1 | 1 | |
| **ADCS** | | | | | | | | | | | | | | | | | | | | 1 | 1 | |
| **Telecom** | | | | | | | | | | | | | | | | | | | | 1 | 1 | |
| **Power** | | | | | | | | | | | | | | | | | | | | 2 | 1 | |
| **Propulsion** | | | | 4 | | | | | | 3 | | | | | | | | | | 1 | 1 | |
| **Thermal** | | | | | | | | | | | | | | | | | | | | 1 | 1 | |
| **Mechanical** | | | | | | | | | | | | | | | | | | | | | 2 | |
| **MEL** | | | | 1 | 2 | 1 | | | | | | | | | | | | | 2 | 2 | | |
| **Timeline** | | | | | | | | | | | | | | | | | | | | | | |

**Figure 4. A design structure matrix (DSM) for the round-trip SEP MSR orbiter model. Each row or column represents a separate domain-specific sub-model. Each cell represents a link or dependency from the element listed on a row to the element listed on the column. The value in the cell indicates the number of links between the models. The red region represents the mission design models. The blue region represents the models responsible for the margin calculations. The green region represents the models responsible for the spacecraft subsystem sizing.**

some of the data included in the database. The figure shows a contour plot of mass delivered to a low-Mars science orbit versus flight time from launch to orbit with each contour representing a different power level. Launch is in 2022 and one BPT-4000 Hall-effect thruster is assumed.

The outbound trajectory model interpolates among the various trajectories in the database to estimate a trajectory for a given set of inputs. The user may set the launch year, launch vehicle, and number of thrusters as constant parameters. The model requires inputs of the solar array power at 1 AU and the spacecraft arrival mass at Mars. The required Xenon (propellant) mass for

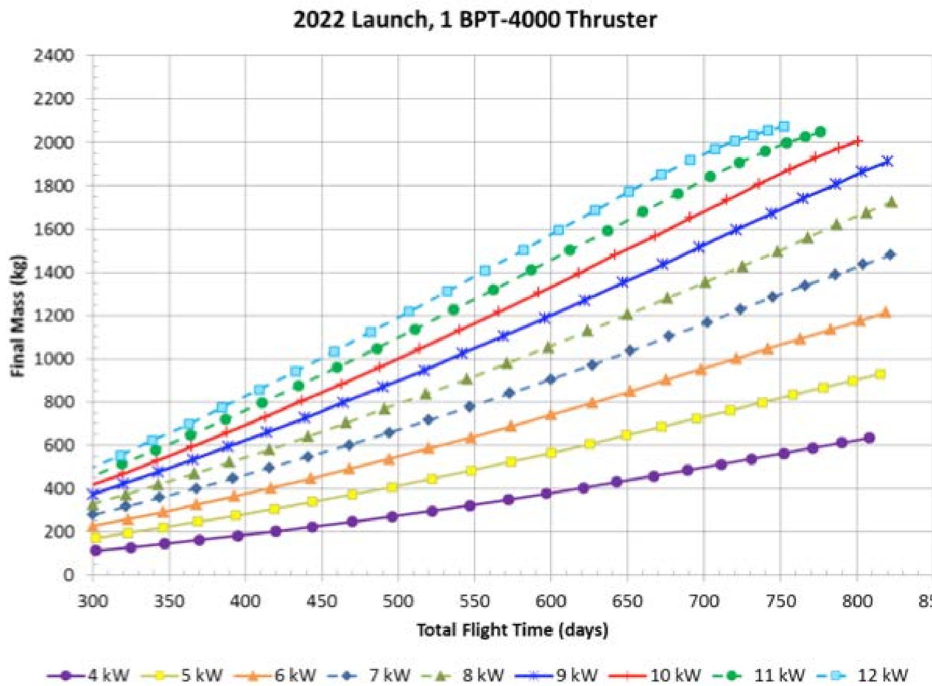


**Figure 5. Mass delivered to a Mars Science Orbit vs. Total Flight Time for 1 BPT-4000 Thrusters Launching in 2022. A Falcon 9 launch vehicle is assumed.[11]**

a given trajectory is determined by linear interpolation between the closest adjacent MALTO runs in the database. Other outputs of the model, similarly determined through interpolation, are: characteristic launch energy ($C_3$), launch date, cruise propellant vs. spiral propellant (percentage), and TOF.

**Mars-to-Earth (Inbound) Trajectories**

Similar to the outbound trajectory model, the inbound trajectory model is based on interpolation of a database of MALTO trajectories computed across a number of return years. While the outbound trajectories include a constraint on departure mass due to launch vehicle performance, the inbound trajectory set has an additional free parameter (departure mass) but is constrained to depart Mars with $C_3$=0 km$^2$/s$^2$. The inbound trajectories include scans across return year, number of thrusters, power level, and mass delivered to Earth (500, 1000, and 1500 kg). From this set of trajectories, we developed a response surface that estimates propellant (Xenon) mass and TOF vs. inputs of arrival mass and power level.

Response surface curves were fit to databases of Mars-to-Earth trajectories for 2026 and 2028 return opportunities. To develop these curve fits, the Xenon mass fraction ($M_{Xe}/M_{Dry}$) was plotted vs. TOF. Points closest to the origin (i.e. minimum TOF & propellant mass fraction) were used for further analysis. A power-law correlation was found between the mass, power, and propellant mass fraction. Equation (7) gives the curve fit for Xenon mass.

$$M_{Xe} = \left(\beta_1 P^{\beta_2} + \beta_3\right) M_{Dry} \tag{7}$$

Equation (8) gives the curve fit for TOF as a function of spacecraft dry mass ($M_{Dry}$), and Power (P).

$$TOF = \left(\beta_1 P^{\beta_2} + \beta_3\right)\left(\beta_4 + \beta_5 M_{Dry}\right) + \beta_6 M_{Dry} + \beta_7 \tag{8}$$

The curve fit parameters for these two equations were found for the Mars departure years of 2026 and 2028 for a 1 thruster case, and are shown in Table 1.

**Table 1. Curve fit parameters for inbound trajectory data by return year**

| Return Year | 2026 | 2028 |
|---|---|---|
| $\beta_1$ | 1.876 | 1.793 |
| $\beta_2$ | -1.363 | -1.294 |
| $\beta_3$ | 0.293 | 0.282 |
| $\beta_4$ | 457.1 | 444.0 |
| $\beta_5$ | 1.603 | 1.705 |
| $\beta_6$ | -0.340 | -0.383 |
| $\beta_7$ | 81.8 | 114.4 |

The outbound trajectory model takes inputs of power and spacecraft mass delivered to Earth (defined as dry mass plus any residual fuel), and returns a xenon propellant mass and a TOF.

**ΔV Calculator**

The ΔV calculator included in the tool is responsible for combining the outputs from the outbound and inbound trajectories, along with other ΔV allocations to determine a total propellant requirement for the spacecraft. These propellant outputs are fed into other subsystem models (propulsion, mechanical, MEL, etc.) to converge on a feasible spacecraft design. An example ΔV calculation for a 2022 launch, 2028 return, single BPT-4000 round-trip SEP orbiter (corresponding to the left-most column in Table 4) is shown in Table 2.

The inbound & outbound spiral & cruise Xenon masses in Table 2 are taken as inputs from the inbound and outbound trajectory models; the corresponding ΔVs are calculated based on a constant SEP thruster $I_{sp}$ and these masses. The delivered dry mass is given as an input from either the MEL or the Mass & Power Margin models. Two other outputs are determined: the Mars arrival mass and the launch mass, both indicated in Table 2. These values are used as inputs to the outbound trajectory model and the launch vehicle models, respectively.

**Table 2. Example ΔV calculation for a 2022 launch, 2028 return, single BPT-4000 round-trip SEP orbiter.**

| Event | ΔV | Prop. System | $I_{sp}$ (s) | Pre-Event Mass (kg) | Δ Mass (kg) |
|---|---|---|---|---|---|
| ***Launch Mass*** | **-** | **-** | **-** | ***2825*** | - |
| **SEP Outbound Cruise Xenon** | 2484 m/s | SEP | 1500 | 2825 | 439 |
| **SEP Outbound Spiral Xenon** | 2530 m/s | SEP | 1500 | 2386 | 377 |
| **Cruise/Spiral ACS, Safe mode** | 19 m/s | ACS Thrusters | 210 | 2009 | 19 |
| *Mars Arrival Mass* | **-** | **-** | **-** | ***1991*** | **-** |
| **Low Orbit Mass Jettison** | - | Mass Add./Jett. | - | 1991 | 0 |
| **Mars Orbit ACS, Safe mode** | 12 m/s | ACS Thrusters | 210 | 1991 | 12 |
| **Orbit Maintenance & EDL Phasing** | 30 m/s | SEP | 1500 | 1979 | 4 |
| **Sample Rendezvous & Capture** | 242 m/s | SEP | 1500 | 1975 | 32 |
| **SEP Inbound Spiral Xenon** | 2432 m/s | SEP | 1500 | 1943 | 296 |
| **SEP Inbound Cruise Xenon** | 2296 m/s | SEP | 1500 | 1647 | 238 |
| **Spiral/Cruise ACS, Safe Mode** | 7 m/s | ACS Thrusters | 210 | 1409 | 5 |
| **Earth Bias Maneuver** | 10 m/s | SEP | 1500 | 1404 | 1 |
| ***Delivered Mass to Earth*** | **-** | **-** | **-** | ***1403*** | **-** |
| **Total Propellant** | 10062 m/s | **Total** | | | 1422 |
| **SEP Xenon Propellant** | 10024 m/s | **SEP** | | | 1387 |
| **ACS Propellant** | 38 m/s | **ACS Thrusters** | | | 35 |

## Margin Implementation in the Orbiter-Sizing Tool

In the orbiter-sizing tool, the three key margin values described in this paper— mass margin, SEP power margin, and propellant margin—are defined as user inputs. As shown in the DSM for the tool in Figure 4, the Outbound Trajectory, Inbound Trajectory, ΔV, and Launch Vehicle models are all run twice through in the model, each set with different inputs. The first set of these four models is run with the un-margined values of spacecraft mass and solar array power, and no propellant margin. After running the models for the un-margined cases, the tool runs the Power & Mass Margin and Propellant Margin models. The Power & Mass Margin model determines the margined spacecraft dry mass, $M_{Dry,MEV}$, from Equation (1), and the margined power available for SEP, $P_{SEP}^{M}$, from Equation (4). These margined mass and power values are fed as the inputs to the second set of ΔV, Trajectory, and Launch Vehicle models, which report a propellant mass and other figures-of-merit for the margined spacecraft. In this way, the tool can report both the un-margined and margined performance for a given spacecraft design.

# MSR ORBITER ARCHITECTURES

Architecture options for SEP MSR orbiters are similar in many respects to previous chemical science and MSR spacecraft architectures for Mars. The SEP architectures differ in the addition of functions for science and telecom relay while at Mars, and longer Mars stay times to accommodate multiple launch opportunities for the Sample Retrieval Lander mission as well as the details of trajectory, propulsion, and power generation. Single and multiple spacecraft architectures with varying division of functions are possible and offer a variety of benefits and constraints. Because SEP missions for MSR have grown in interest recently, three basic architecture options have been examined and example missions are compared using the SEP orbiter-sizing tool described in this paper. The orbiter architectures are fully redundant and are single fault tolerant. Lifetime expectations are 5-10 years. Power, data storage, ΔV, and telecommunications data rates are determined consistent with mission use scenarios and these are reflected in the mass estimates via subsystem component sizing.

The basic reference mission architecture, option 1, is a single, round-trip orbiter. The round-trip orbiter performs all desired mission functions. After arrival, the orbiter performs science observations and telecom relay functions while waiting, perhaps for years, for the orbiting samples (OS) to be launched from Mars' surface. The orbiter locates the OS, captures it, and transfers it to an Earth Entry Vehicle (EEV). The orbiter then departs Mars to return to Earth.

Option 2 features a one-way orbiter that delivers a sample return orbiter "daughter-craft" to Mars orbit, captures the OS, transfers it to an Earth Entry Vehicle (EEV) on the daughter-craft, and then stays behind to continue science and telecom relay functions while the daughter-craft returns to Earth.

Option 3 features a round-trip or "host" orbiter that carries a science daughter-craft to Mars. The science daughter-craft contains the rendezvous, capture, sample handling, science, and data relay payload elements. These payload elements are operated by the host orbiter to collect the OS and transfer it to the EEV. The science daughter-craft is then deployed in low Mars orbit to continue operations at Mars and the host orbiter departs Mars to return to Earth.

Payload mass allocations are common across all architecture options and mission examples. The 190 kg payload is comprised of 110 kg for orbiting sample (OS) capture and handling equipment, 10 kg for OS rendezvous sensing instruments, and 70 kg for complementary science instruments. 15 kg of UHF relay communications equipment is assumed as part of telecommunications subsystems for all orbiters that remain in Mars orbit for extended periods. These payload elements are applied consistently and as needed across all architecture elements.

The relative system sizing of these three architectures is shown below to show the versatility of the modeling methods. Elaboration on the relative benefits to the mission goals will be left for future work.

**Example MSR Orbiter Cases**

Using the orbiter-sizing tool, examples have been developed for each of the architecture options. Multiple examples of some of the options are shown to highlight some system-level tradeoffs and consequences.

Several key input parameters used in the orbiter-sizing tool for this comparison are shown in Table 3. These inputs determine the architecture options and parameters for a study. Detailed subsystem models can be altered to support the needs of specific mission cases.

**Table 3. Key trajectory and spacecraft input parameters for MSR orbiter sizing tool**

| Input Parameter | Range | Description |
|---|---|---|
| *Outbound Trajectory* | | |
| Launch Year | 2022, 2024, 2026 | Launch year from Earth |
| Number of Thrusters | 1 or 2 | Assume BPT-4000 thruster |
| Power Level | 4 – 20 kW | Power at 1 AU, EOL equivalent |
| Launch Vehicle | Falcon 9 v1.1 | LV performance from NLS-II contract used in trajectory optimizer |
| *Inbound Trajectory* | | |
| Return Year | 2026, 2028 | Year to begin spiral-out from Mars |
| Number of Thrusters | 1 or 2 | Assume BPT-4000 thruster (plus one inactive redundant thruster) |
| Power Level | 4 – 20 kW | Power at 1 AU, EOL equivalent |
| *Campaign* | | |
| MSR Lander Launch Date | 2022, 2024, 2026, 2028 | Used for estimating MSR campaign timeline; ballistic lander trajectories assumed |
| *Spacecraft* | | |
| Number of Spacecraft | 1 or 2 | Round-trip orbiter or single direction orbiter with daughter-craft |
| Solar Array Design Power | 4 – 20 kW | Power at 1 AU, EOL equivalent for entire solar array. Must be greater than or equal to outbound or inbound trajectory power |
| Payload Mass | 0 – 500 kg | Science and sample-return payload. Set to 190 kg for all options. |
| Avg. Spacecraft Bus Power | 700 W | Spacecraft bus power, not including SEP power, but including bus power margin |
| Subsystem Reference Design (separate inputs for each sub-system) | MRO, MAVEN, InSight, DAWN, Odyssey | C&DH, Telecom, ADCS, Power, and Thermal sub-system dry masses are chosen by analogy from heritage spacecraft |
| Additional Propulsion Tank Capacity | 0 – 500 kg | Extra tank mass is estimated from additional propellant capability required |

A wide variety of data can be extracted from the sizing tool. Several key figures-of-merit (FOM) for the round-trip MSR orbiter include: propellant throughput, launch mass (spacecraft wet mass), neutral mass (dry mass plus allocated propellants), mass margin, power margin, total TOF (outbound & inbound), and orbiter duration at Mars.

A timeline module is included in the orbiter-sizing tool. This module includes the TOF, launch date, and arrival date estimates from the outbound trajectory and inbound trajectory modules. An example output of the timeline module for a 2020 orbiter launch case and comparing MSR lander launches in 2024 and 2026 is shown in Figure 6. One of the key figures-of-merit, the duration available for MSR activities, is the difference between the lander arrival date and the Mars departure date.

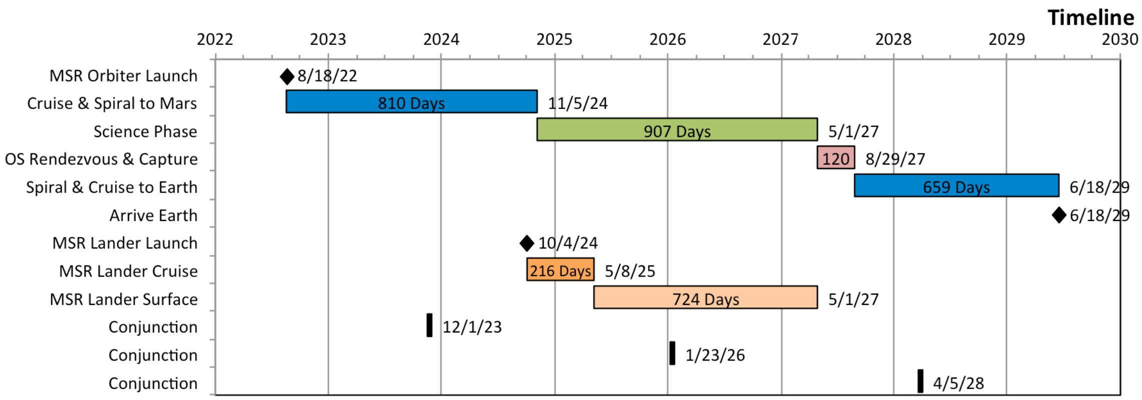


**Figure 6. MSR Campaign Timeline for 2022 Orbiter Launch and 2024 Lander Launch**

The mass outputs from the orbiter-sizing tool for the example MSR orbiter cases are very conservative. The subsystem models are derived from analogy-based estimates from historical or late-development Mars and SEP spacecraft (Odyssey, MRO, DAWN, MAVEN, InSight, & SMAP). No attempt has been made to assess the effects of margin consumption in these subsystems to meet mission specific trades and constraints. The tool then adds a standard JPL margin of 43% to the mass estimate in the Power & Mass Margin model. The resulting system mass and propellant estimates are higher than they would be for detailed mission studies. This conservatism, however, is equally applied to all comparative studies. The impact of this conservative mass is higher fuel requirements and longer trip times to and from Mars (about 30% each). Future work will focus on creating subsystem models that have appropriate maturity for the applied system margin.

A summary of the mass outputs from the orbiter-sizing tool for the example orbiter cases is shown in Table 3. Each of the architecture types is sized for the same mission parameters: 2022 launch, 2028 Mars departure, 190 kg payload, and 700W margined bus average power consumption. For each architecture option, two variations are considered – a single thruster configuration and a dual thruster configuration. The BPT-4000 Xenon throughput is theoretically limitless, however the throughput qualification is currently planned to extend to 600 kg. For a given mission option, throughput qualification could be traded for additional thruster strings. This is further compounded with the choice of using the additional thrusters sequentially for throughput extension or simultaneously for additional thrust (and the added power system size for that thrust). Table 4 shows the impacts of several of these trades, which can be observed by comparing the columns.

**Table 4. Comparison of three families of MSR orbiter configurations: round-trip orbiter, one-way orbiter carrying a return daughter-craft, and a round-trip orbiter carrying a science daughter-craft. These designs are shown for a launch year of 2022 and a return year of 2028 with both 1 and 2 thruster cases.**

| Parameter | *Option 1* | | *Option 2* | | | *Option 3* | |
|---|---|---|---|---|---|---|---|
| | **Round-Trip Orbiter** | **Round-Trip Orbiter** | **One-Way Orbiter + Daughter Return** | **One-Way Orbiter + Daughter Return** | **Daughter-Craft Return Orbiter** | **Round-Trip + Science Daughter** | **Round-Trip + Science Daughter** |
| Number of Thrusters | 1 | 2 | 1 | 2 | 1 | 1 | 2 |
| Launch Mass (MEV) | 2825 kg | 3411 kg | 3456 kg | 3976 kg | 1183 kg | 3215 kg | 3784 kg |
| Xe Mass | 1387 kg | 1722 kg | 844 kg | 1126 kg | 352 kg | 1364 kg | 1693 kg |
| Chem Prop Mass | 35 kg | 41 kg | 43 kg | 49 kg | 21 kg | 44 kg | 51 kg |
| Carried Mass | 0 kg | 0 kg | 1183 kg | 1183 kg | 0 kg | 465 kg | 465 kg |
| System Mass Margin | 422 kg | 496 kg | 417 kg | 487 kg | 244 kg | 403 kg | 474 kg |
| S/C Dry Mass (CBE) | 981 kg | 1153 kg | 969 kg | 1132 kg | 567 kg | 939 kg | 1101 kg |
| P/L Mass | 190 kg | 190 kg | 150 kg | 150 kg | 40 kg | 120 kg | 120 kg |
| Launch $C_3$ | 8.5 $km^2/s^2$ | 3.5 $km^2/s^2$ | 8.5 $km^2/s^2$ | 3.5 $km^2/s^2$ | - | 8.5 $km^2/s^2$ | 3.5 $km^2/s^2$ |
| Launch Vehicle | Falcon 9 v1.1 | Atlas V 411 | Atlas V 421 | Atlas V 421 | - | Atlas V 411 | Atlas V 421 |
| Array Power EOL at 1 AU | 12 kW | 20 kW | 12 kW | 20 kW | 10 kW | 12 kW | 20 kW |
| Launch Year | 2022 | 2022 | 2022 | 2022 | - | 2022 | 2022 |
| Return Year | 2028 | 2028 | - | - | 2028 | 2028 | 2028 |
| Earth-Mars SEP Duration | 809 days | 670 days | 809 days | 670 days | - | 809 days | 670 days |
| Mars-Earth SEP Duration | 659 days | 637 days | 547 days | 547 days | 547 days | 664 days | 678 days |
| Total SEP Duration | 1468 days | 1307 days | 1356 days | 1217 days | 547 days | 1473 days | 1348 days |
| Time at Mars | 1027 days | 1214 days | 1135 days | 1301 days | | 1043 days | 1230 days |
| Mass Margin | 43% | 43% | 43% | 43% | 43% | 43% | 43% |
| Pwr. Margin | 30% | 30% | 30% | 30% | 30% | 30% | 30% |

**Key Findings for the Orbiter Cases**

In option 1, the round-trip orbiter case performs well for a single thruster option in all aspects except throughput. The power system is near saturation, meaning that adding more power would not increase performance significantly because the engine operates at nearly full power for the whole mission. This configuration fits within the expected performance of the SpaceX Falcon-9 v1.1, even with conservative mass margins. The 2-thruster case also performs well but still well above the planned throughput qualification levels. It is a larger and more complex spacecraft design and fits within an Atlas V 411[*] performance envelope and could accommodate additional mass.

[*]The outbound trajectories used in the tool were optimized for the Falcon 9 v1.1 launch mass capability. If an orbiter exceeds the launch mass capability of the Falcon 9 v1.1, it is shown on the next largest launch vehicle on which it fits for the required $C_3$. Further trajectory analysis optimized for the Atlas V launch vehicle family needs to be done and incorporated into the orbiter-sizing tool to take advantage of the capabilities of launch vehicles in this class.

The option 2, one-way orbiters with daughter-craft return orbiter, cases perform well on an Atlas V 421 with conservative margins. The outbound one-way orbiters are comparable in size and mass to their round-trip counterparts. Xenon throughput is lower, however and the 2-thruster case is within planned qualification testing. The daughter-craft fits well within all desired parameters and with conservative margins. Total mission duration is shorter and time at Mars is longer as the daughter-craft is lighter, enabling a shorter duration inbound trajectory.

The option 2, round-trip orbiters with science daughter-craft, cases also perform well on an Atlas V 421 with conservative margins. These round-trip orbiters are comparable in size, mass, and throughput to their basic round-trip counterparts in option 1. The carried science daughter-craft drives the launch vehicle size to the Atlas V 421.

For previous MSR mission concepts using chemical propulsion and ballistic trajectories with aerobraking, launch masses were comparable to the SEP mission described in this paper but $C_3$ values were much higher (11-17 $km^2/s^2$ vs. 3.5-8.5 $km^2/s^2$), requiring larger family Atlas V launch vehicles (531-551).[18] They also did not carry science payloads and attendant high data-rate processing and telecommunication subsystems. Chemical ballistic trajectories generally have shorter trip times than for SEP missions by about 20%.

## SENSITIVITY ANALYSES

The orbiter-sizing tool we have developed allows the user to vary many input parameters and evaluate their sensitivity. This section demonstrates what types of sensitivity analyses are possible with examples of varying the number of thrusters and the launch year. These two sensitivity studies demonstrate only a fraction of the capability of the orbiter-sizing tool's ability to examine this class of SEP Mars Sample Return orbiter.

### Number of Thrusters

In Table 4, three orbiter architectures are shown, each with a one- and two- thruster configuration. Based on this data, the average additional spacecraft dry mass due to adding a thruster is ~165 kg; the average additional Xenon propellant mass is ~315 kg. The mass of a thruster string is about 50 kg. The rest of the mass increase is from wraps on the other subsystems for the additional mass, increases in system mass margin, and tankage for additional fuel for the increased mass. The additional Xenon is needed to move the additional mass to and from Mars. In general, adding a SEP thruster to a spacecraft would decrease the TOF to and from Mars; in the cases shown here, the decrease in TOF to Mars is approximately 4 months.

### Launch Year

Due to the differences in orbital position of Mars and Earth in different synodic periods, the launch energy required for a ballistic trajectory will differ. SEP has the ability to eliminate much of this variability. We ran the single-thruster round-trip orbiter case over five launch opportunities from 2018 to 2026, and recorded the margined spacecraft dry mass and the total propellant mass required for each year. The results are plotted in Figure 7. Over this period, the margined spacecraft dry mass varies by less than 25 kg. The total propellant required varies by approximately 100 kg, with only a 50 kg variation if the 2018 launch opportunity is ignored.

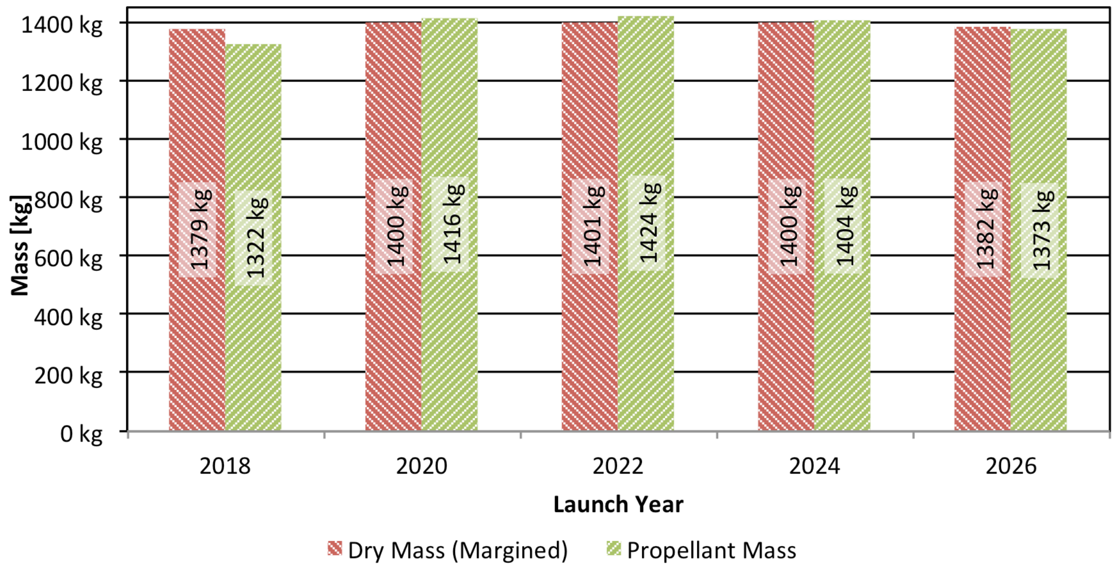


**Figure 7. Variation in margined spacecraft dry mass and propellant mass over five launch opportunities from 2018 through 2026**

## CONCLUSIONS

We have developed a new MSR orbiter-sizing tool that can be used to rapidly explore the trade space of possible designs, and conduct sensitivity studies on these designs. We have architected this tool to include the ability to design SEP spacecraft with robust mass, power, and propellant margins.

Using this tool, we find that a wide variety of system designs are possible for MSR orbiters. These orbiter designs allow much more dry mass capability than a chemical orbiter option for a given launch vehicle. This additional mass capability could be used to accommodate a daughtercraft, greatly increasing the flexibility of the mission for science return and other infrastructure services at Mars. The variability in mass capability between launch opportunities is greatly reduced by using SEP.

## FUTURE WORK

More work is needed to more clearly understand the impact of including large margins in mass, power, and propellant for SEP missions. Using the tool we have developed, we would like to perform a Monte Carlo analysis to see how different distributions of mass, power, and propellant growth interact in a SEP spacecraft.

Additional work is needed to understand the amount of conservatism and implied mass margin included in the spacecraft subsystem models. We plan to implement a new interpolation method for the outbound and inbound trajectory models. Finally, we plan to continue using the model to refine current MSR orbiter concepts and investigate new ones.

## ACKNOWLEDGMENTS

This work was conducted at the Jet Propulsion Laboratory, California Institute of Technology. Government sponsorship is acknowledged. The authors would like to thank Tom Randolph, Steve Snyder, David Oh, and Richard Hofer for their help understanding margins for SEP spacecraft.

## REFERENCES

[1] National Research Council, *Vision and Voyages for Planetary Science in the Decade 2013-2022*, Washington, D.C: National Academies Press, 2011.

[2] Mustard, J. F., Adler, M., Allwood, A., Bass, D. S., Beaty, D. W., III, J. F. B., Brinckerhoff, W. B., Carr, M., Des Marais, D. J., Drake, B., Edgett, K. S., Eigenbrode, J., Elkins-Tanton, L. T., Grant, J. A., Milkovich, S. M., Ming, D., Moore, C., Murchie, S., Onstott, T. C., Ruff, S. W., Sephton, M. A., Steele, A., and Treiman, A., *Report of the Mars 2020 Science Definition Team*, Mars Exploration Program Analysis Group (MEPAG), 2013.

[3] Mattingly, R., and May, L., "Mars Sample Return as a Campaign," *2011 IEEE Aerospace Conference*, Big Sky, MT: IEEE, 2011.

[4] O'Neil, W. J., and Cazaux, C., "The Mars Sample Return Project," *Acta Astronautica*, vol. 47, Jul. 2000, pp. 453–465.

[5] Rayman, M. D., and Williams, S. N., "Design of the First Interplanetary Solar Electric Propulsion Mission," *Journal of Spacecraft and Rockets*, vol. 39, Jul. 2002, pp. 589–595.

[6] Racca, G. D., Whitcomb, G. P., and Foing, B. H., "The SMART-1 Mission," *ESA Bulletin*, vol. 95, 1998, pp. 72–81.

[7] Kawaguchi, J., Kuninaka, H., Fujiwara, A., and Uesugi, T., "MUSES-C, Its Launch and Early Orbit Operations," *Acta Astronautica*, vol. 59, Oct. 2006, pp. 669–678.

[8] Rayman, M. D., Fraschetti, T. C., Raymond, C. A., and Russell, C. T., "Dawn: A Mission in Development for Exploration of Main Belt Asteroids Vesta and Ceres," *Acta Astronautica*, vol. 58, Jun. 2006, pp. 605–616.

[9] Oh, D. Y., Hofer, R. R., Katz, I., Sims, J. A., Warner, N. Z., Randolph, T. M., Reeve, R. T., and Moeller, R. C., "Benefits of Using Hall Thrusters for a Mars Sample Return Mission," *The 31st International Electric Propulsion Conference*, University of Michigan, USA: 2009.

[10] Landau, D., Chase, J., Randolph, T., Timmerman, P., and Oh, D., "Electric Propulsion System Selection Process for Interplanetary Missions," *Journal of Spacecraft and Rockets*, vol. 48, May 2011, pp. 467–476.

[11] Hofer, R., "AIAA Electric Propulsion Short Course, Chapter 8: Hall Thrusters," Jan. 2012.

[12] Mathers, A., De Grys, K., and Paisley, J., "Performance Variation in BPT-4000 Hall Thrusters," *31st International Electric Propulsion Conference, IEPC-2009-144, Ann Arbor, MI*, 2009, IEPC–2009–144.

[13] Kowalkowski, T. D., Bailey, Z. J., Lock, R. E., Sturm, E. J., and Woolley, R. C., "Robotic Mars Exploration Trajectories Using Hall Thrusters," *24th AAS/AIAA Space Flight Mechanics Meeting*, Santa Fe, NM: AAS, 2014, AAS 14–364.

[14] Sims, J., Finlayson, P., Rinderle, E., Vavrina, M., and Kowalkowski, T., "Implementation of a Low-Thrust Trajectory Optimization Algorithm for Preliminary Design," American Institute of Aeronautics and Astronautics, 2006.

[15] Rayman, M. D., Fraschetti, T. C., Raymond, C. A., and Russell, C. T., "Coupling of System Resource Margins Through the Use of Electric Propulsion: Implications in Preparing for the Dawn Mission to Ceres and Vesta," *Acta Astronautica*, vol. 60, 2007, pp. 930 – 938.

[16] Oh, D. Y., Snyder, J. S., Goebel, D. M., Hofer, R. R., Landau, D. F., and Randolph, T. M., "Solar Electric Propulsion for Discovery Class Missions," *33rd International Electric Propulsion Conference*, The George Washington University, Washington, D.C.: 2013, IEPC–2013–124.

[17] Oh, D., Landau, D., Randolph, T., Timmerman, P., Chase, J., Sims, J., and Kowalkowski, T., "Analysis of System Margins on Deep Space Missions Using Solar Electric Propulsion," *44th AIAA/ASME/SAE/ASEE Joint Propulsion Conference & Exhibit*, Hartford, CT: 2008.

[18] Lock, R. E., Bailey, Z. J., and Kowalkowski, T. D., "Mars Sample Return Orbiter Concepts Using Solar Electric Propulsion for the Post−Mars2020 Decade," *2014 IEEE Aerospace Conference*, Big Sky, MT: IEEE, 2014.